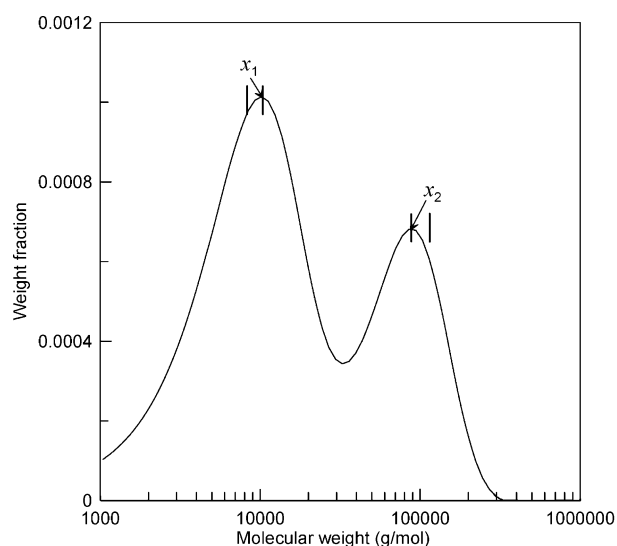


“Living” Radical Polymerization in Tubular Reactors, 2 – Process Optimization for Tailor-Made Molecular Weight Distributions

Mariano Asteasuain,* Matheus Soares, Marcelo K. Lenzi, Robin A. Hutchinson, Michael Cunningham, Adriana Brandolin, José Carlos Pinto, Claudia Sarmoria

“Living” radical polymerization is a relatively new polymerization process that can be used to prepare resins with controlled structures. In this work, a mathematical model developed previously to describe nitroxide-mediated “living” radical polymerizations performed in tubular reactors is used for the optimization of the process and obtainment of tailor-made MWDs. Operating conditions and design variables are determined with the help of optimization procedures in order to produce polymers with specified MWDs. It is shown that bimodal and trimodal MWDs, with given peak locations, can be obtained through proper manipulation of the operating conditions. This indicates that the technique discussed in this work is suitable for detailed design of the MWD of the final polymer.



M. Asteasuain, C. Sarmoria, A. Brandolin
Planta Piloto de Ingeniería Química (Universidad Nacional del Sur – CONICET), Camino La Carrindanga km. 7, 8000 Bahía Blanca, Argentina
Fax: +54 291 486 1600; E-mail: masteasuain@plapiqui.edu.ar
M. Soares, J. C. Pinto
Programa de Engenharia Química/COPPE, Universidade Federal do Rio de Janeiro, Cidade Universitária, CP: 68502, Rio de Janeiro 21945-970, RJ, Brazil
M. K. Lenzi
Universidade Federal do Paraná, Departamento de Engenharia Química, Setor de Tecnologia – Jardim das Américas, Caixa Postal 19011, 81531-990 Curitiba, Paraná, Brazil
R. A. Hutchinson, M. Cunningham
Department of Chemical Engineering, Queen’s University, Dupuis Hall, 19 Division Street, Kingston, ON K7L 3N6, Canada

Introduction

“Living” or controlled radical polymerization is a relatively new polymerization process that can be used to prepare resins with controlled structures. It combines the advantages of conventional free radical polymerization and traditional living polymerization techniques, such as easy operation and the narrow molecular weight distributions of the obtained polymer resins. Resins with controlled structures can be synthesized through this reaction mechanism, with the advantage of a more flexible and versatile route than traditional living polymerization.

The controlled growth of polymer chains in “living” radical polymerizations is achieved through addition of an agent that causes the reversible termination or transfer

reactions, leading to alternating periods of inactivity and normal activity of the growing polymer chains. As in typical free radical polymerizations, several monomers can be polymerized and the presence of impurities, such as water and oxygen, is tolerated. “Living” radical polymerization can also be used to perform heterogeneous polymerizations, such as emulsion, suspension or dispersion polymerizations.

There are several variants of controlled free radical polymerization. The main ones are atom transfer radical polymerization (ATRP), reversible addition-fragmentation chain transfer (RAFT), and nitroxide-mediated living polymerization (NMLP).^[1,2] In ATRP and NMLP, a dynamic equilibrium is established between a small number of growing radicals and a large quantity of inactive chains by means of a reversible termination. Inactive chains are usually alkyl halides in ATRP and alkoxyamines in NMLP.^[2] On the other hand, RAFT is based on a rapid transfer reaction between active and dormant chains. As a result, radical concentration is (ideally) not affected, but is determined by the rate of initiation-termination reactions, as in conventional free radical polymerization. In practice however, retardation or inhibition is frequently observed. A detailed discussion of these mechanisms may be found elsewhere.^[1–4]

The molecular weight distribution (MWD) is one of the most important polymer properties. Its shape (i.e., position, width, height, number of peaks and shoulders, etc.) determines many of the end-use and processing properties of the material. For some special applications, wide or even multimodal MWDs may be required because the low molecular weight polymer acts as a flow promoter, while the high molecular weight chains improve the mechanical properties.^[5–12] “Living” radical polymerization can be used for producing polymers with narrow MWD at different molecular weight ranges or even multimodal MWDs, by changing the operating conditions or the reactor configuration.^[5,13] Several mathematical models have been developed for the different “living” radical polymerization processes,^[14] which have focused mainly on average molecular properties.^[14] Although a few efforts at optimizing this process have been published,^[15] none of them involved tailoring of the MWD shape.

Nowadays “living” radical polymerization processes are carried out mainly in batch or semibatch operation. However, as this type of operation is discontinuous, important delays in production are introduced, reducing productivity. On the other hand, the use of continuous tubular reactor processes shows great potential because of their capability to influence the polymer molecular structure by proper manipulation of the operating conditions. For instance, control of the polymer structure can be simplified by using feed streams located along the reactor. In this way, the conversion at which the additional

reactants are added can be easily adjusted by varying the flow rate. Besides, it is possible to achieve a good control of the temperature profile, and operation under pressure is easier than in a tank reactor. However, the study of “living” radical polymerization in tubular reactors, either theoretically or experimentally, has seldom been performed.

Enright et al.^[16] carried out nitroxide-mediated “living” radical polymerizations (NMLP) of styrene in tubular reactors and showed the feasibility of this technology, which allowed them to obtain stable latexes with minimum coagulum formation. They found that polymerization kinetics in the tubular reactor was similar to that in a batch reactor. Zhang and Ray^[13] developed a mathematical model for a tubular reactor with axial dispersion, and compared model predictions with experimental data obtained in batch reactors. They analyzed the influence of the Peclet number and presented simulation results, showing that bimodal distributions can be obtained by introducing side feedings to the reactor. However, they employed a simple method for predicting the MWD that can only be applied under certain conditions. They did not attempt to design the polymer MWD. Russum^[17] performed a theoretical and experimental analysis of reversible addition-fragmentation chain transfer (RAFT) in tubular reactors, analyzing the effects of flow regime in the polymer properties. He found that the reaction kinetics in a tubular reactor was similar to the kinetics observed in batch tank reactors. However, the polydispersity of the polymer produced in the tubular reactor was consistently higher than that produced in concurrent batch experiments, suggesting a contributing role of axial dispersion. Noda et al.^[18] carried out homo- and copolymerizations of methyl methacrylate (MMA) in a tubular reactor, analyzing the effects of flow rate, temperature and monomer/initiator ratios. They found that the tubular reactor was appropriate for the synthesis of block copolymers, where the block length was varied through the flow rates of the comonomers. Their results also suggested that this continuous system could be applied for various ATRP systems. Faliks et al.^[15] carried out an optimization of a NMLP process in a tubular reactor, but they focused only on average molecular properties.

In a previous work,^[19] we presented a mathematical model for a nitroxide-mediated “living” radical polymerization (NMLP) performed in a tubular reactor. This model considers the variation of physical and transport properties along the axial distance and is able to predict the complete MWD, regardless of its shape. Besides, the proposed model is efficient for implementation of optimization problems. In the study presented here, the previously proposed model is used for optimization of the process in order to obtain tailor-made MWDs. Operating conditions and design variables, such as reactor temperature, monomer, initiator and capping agent flow rates, as

well as the positions of the lateral feeds, are determined so as to produce polymer materials with specified MWDs. Focus is placed in designing the process for achieving bimodal and even trimodal MWDs, with requirements on the location and height of the distribution peaks.

Process Description and Optimization Aspects

The tubular reactor analyzed here and used to perform the NMLP has a main feed consisting of peroxide initiator (benzoyl peroxide, BPO), styrene and 2,2,6,6-tetramethylpiperidyl-1-oxy (TEMPO). This nitroxide compound acts as a capping agent, causing the reversible termination that leads to periods of inactivity alternating with periods of normal activity. In this way, the concentration of growing radicals is kept at very low values, minimizing bimolecular termination reactions. Besides, macroradicals are, on average, half of the time active and half of the time inactive. In this way, all polymer chains grow at almost the same rate, resulting in low polydispersity indexes. As this polymerization mechanism produces narrow molecular weight distributions, it is possible to obtain multimodal MWDs in a tubular reactor by means of lateral feeds, through which new polymeric chains are initiated. Polymer of different molecular weights can be produced by controlling the growth of each chain population through proper manipulation of the corresponding feed rates of styrene, BPO and TEMPO, resulting in a multimodal MWD at the reactor exit.

The mathematical model of the tubular reactor was presented in Part I of this work.^[19] Briefly, the model assumes plug flow and considers variation of the reaction mixture density and velocity along the axial distance. Although the actual flow pattern would not be plug flow, previous works^[20,21] have shown that this assumption allows accurate model outputs to be achieved for the operating conditions considered in this work. The reaction steps considered in the kinetic mechanism are: initiation by peroxide decomposition, monomer thermal initiation, capping and uncapping reactions, propagation, transfer to monomer, termination by combination and disproportionation involving nitroxide. The complete MWD is computed by means of the probability generating function (pgf) technique.^[22–24] Other model outputs include monomer conversion and concentration of reactants and product. Average molecular weights are also calculated employing the method of moments. Since uniform reactor temperature is considered, the energy balance is not included; however, the energy balance could be easily incorporated if necessary. This particular temperature profile can actually be obtained in the experimental reactor setup represented in this work. The reactor model

was validated using both published data and experimental data obtained from a tubular reactor in our labs. It was shown that the reactor model produced accurate predictions of the complete MWD, monomer conversion and average polymer properties for several sets of operating conditions. It was also shown that the model was efficient for its use in optimization tasks.

The benefits of the pgf technique for modeling the complete MWD were also exemplified in Part I of this work. It is ideal for modeling complex distribution shapes, such as multimodal MWDs, because it does not assume any shape for the distribution. Besides, this method is appropriate for models used in optimization problems, because the size of the model can be tailored to the particular requirements of a given optimization problem, reducing the computational time. For instance, if the process requirement regarding the polymer MWD is only to have a maximum or a minimum in the interval $x_i \pm a$, it is of no use to have a detailed description of the MWD, which generally involves chain lengths values between 1 and 10^3 – 10^5 or more. Actually, only three points of the distribution are required: $h(x_i)$, $h(x_i + a)$ and $h(x_i - a)$, where $h(x_i)$ is the MWD at chain length x_i . A maximum in the interval $x_i \pm a$ can be ensured by including the constraints shown in Equation (1) and (2) in the design problem:

$$h(x_i - a) < h(x_i) \quad (1)$$

$$h(x_i + a) < h(x_i) \quad (2)$$

If a is set to 1, these constraints enforce a maximum at the chain length x_i , because the MWD is an integer distribution and therefore x_i is the only point in the interval $(x_i - 1, x_i + 1)$. This can be used to specify the position of a MWD peak in a design problem. However, the value of $h(x_i)$ is generally very similar to $h(x_i - 1)$ and $h(x_i + 1)$. Hence including the above constraints with $a = 1$ when solving, for instance, an optimization problem may cause numerical difficulties. This can be avoided by setting a to a small integer greater than 1, but still small enough so that x_i can be considered a good approximation of the position of the maximum that will actually be in the interval $(x_i - a, x_i + a)$. In the case of a minimum, the operator “<” in Equation (1) and (2) is replaced by “>”.

The pgf method allows the calculation of any point of the MWD independently of any other. Therefore, it is possible to solve the MWD only for the required points. This is an important issue, because the size of the model is proportional to the number of calculated points of the MWD. Continuing with the previous example, even in the case that the required position of the maximum or the minimum (x_i) is not known in advance, it is still possible to calculate only three points of the distribution at each process simulation (i.e., evaluation of the objective

function at each optimization iteration), provided that x_i is included as an optimization variable, together with Equation (1) and (2) as optimization constraints. A set of three points as described above must be included in the model for each maximum or minimum that will be specified for the MWD.

In the present work, the tubular reactor model is included in an optimization framework for the design of operating conditions for producing polymers with target MWDs of complex shape. A bimodal and a trimodal distribution were selected as case studies. A single lateral feed is considered for the first case, and two lateral feeds for the second. Design variables involve the feed rates of styrene, BPO and TEMPO at the reactor inlet and lateral feeds, the location of the lateral feeds, and the operation temperature. Modeling and optimization activities were carried out in gPROMS (Process Systems Enterprise, Ltd.). In order to comply with the software requirements, lateral feeds were modeled by adding extra terms to the mass balance equations, as described elsewhere.^[25]

In the following section, results for two optimization problems will be shown. In the first one, the process is designed for achieving a polymer with a bimodal molecular weight distribution, with allowed ranges for the distribution peaks. In the second one, the process design aims at obtaining a trimodal MWD by including an extra peak between the two previous ones. The approach described previously is employed to specify the location of the maxima and minima of the distribution, using a value of $a = 5$.

Optimization Problem 1

This optimization problem involved finding the reactor design and operating conditions that would result in a bimodal MWD with the low molecular weight peak (the approximate position, as mentioned before) between chain lengths 85 and 95, and the high molecular weight one between 850 and 1100. These values are in the range of some actual industrial applications of polymers with bimodal distributions.^[7,12] The optimization goal involved maximization of the amount of the high molecular weight polymer (i.e., the height of the second peak of the MWD). Bimodality of the MWD was sought by means of a lateral feed of monomer, initiator and nitroxide to the reactor. Any lateral inlet of initiator and nitroxide generates a new population of "living" chains, which grow together with the already existing ones and compete with them for the available monomer. The number of new chains is approximately equal to the number of added nitroxide molecules. As a result of the different residence times of the two chain populations, a bimodal distribution can be obtained. In order to match the target MWD, many variables have to be carefully selected, namely: the monomer flow rate at the

main and lateral feeds (which govern the residence times of the polymeric chains), the lateral feed position, the BPO and TEMPO flow rates at the two feeds, and the reactor temperature. These variables are not only numerous, but have complex interactions between them. For this reason it is extremely difficult to estimate or find by a trial-and-error procedure the required values for all of them. Hence, an optimization approach like the one employed in this work becomes a powerful tool. The process design problem included as optimization variables all the process variables mentioned above: monomer, BPO and TEMPO flow rates at the main and lateral feeds, the lateral feed position and the reactor temperature. The mathematical formulation of the optimization problem is:

$$\begin{aligned}
 & \max_{z_{lat}, x_1, x_2, f_{St,main}, f_{BPO,main}, f_{TEMPO,main}, f_{St,lat}, f_{BPO,lat}, f_{TEMPO,lat}, T} FO = w(x_2) \\
 & s.t. \\
 & \text{process model} \\
 & w(x_1 - 5) < w(x_1) \quad (a) \\
 & w(x_1 + 5) < w(x_1) \quad (b) \\
 & w(x_2 - 5) < w(x_2) \quad (c) \\
 & w(x_2 + 5) < w(x_2) \quad (d) \\
 & w(x_1) - 3w(x_2) \leq 0 \quad (e) \\
 & w(x_2) - 3w(x_1) \leq 0 \quad (f) \\
 & 85 \leq x_1 \leq 95 \quad (g) \\
 & 850 \leq x_2 \leq 1100 \quad (h) \\
 & 0 \leq z_{lat} \leq 63 \text{ dm} \quad (i) \\
 & \text{conv} \geq 15\% \quad (j) \\
 & 100^\circ\text{C} \leq T \leq 135^\circ\text{C} \quad (k) \\
 & 0.5 \frac{\text{g}}{\text{min}} \leq f_{St,main} \leq 3.5 \frac{\text{g}}{\text{min}} \quad (l) \\
 & 0.0005 \frac{\text{g}}{\text{min}} \leq f_{BPO,main} \leq 0.006 \frac{\text{g}}{\text{min}} \quad (m) \\
 & 0.0001 \frac{\text{g}}{\text{min}} \leq f_{TEMPO,main} \leq 0.005 \frac{\text{g}}{\text{min}} \quad (n) \\
 & 0.2 \frac{\text{g}}{\text{min}} \leq f_{St,lat} \leq 3.5 \frac{\text{g}}{\text{min}} \quad (o) \\
 & 0.0005 \frac{\text{g}}{\text{min}} \leq f_{BPO,lat} \leq 0.01 \frac{\text{g}}{\text{min}} \quad (p) \\
 & 0.0005 \frac{\text{g}}{\text{min}} \leq f_{TEMPO,lat} \leq 0.01 \frac{\text{g}}{\text{min}} \quad (q) \\
 & 1.9 \frac{\text{g}}{\text{min}} \leq f_{St,main} + f_{St,lat} \leq 3.5 \frac{\text{g}}{\text{min}} \quad (r)
 \end{aligned} \quad (3)$$

where $w(x_i)$ is the weight fraction of the overall polymer of chain length x_i ; z_{lat} is the location of the lateral feed; x_1 and x_2 are the chain lengths representing the positions of the first and second peak; and, $f_{St,main}$, $f_{BPO,main}$, $f_{TEMPO,main}$, $f_{St,lat}$, $f_{BPO,lat}$ and $f_{TEMPO,lat}$ are the flow rates of styrene, BPO and TEMPO at the reactor inlet and lateral feed, respectively. Notice that the chain lengths x_1 and x_2 were included as optimization variables, in addition to the optimization variables related to the process design, according to the procedure for specifying the position of the MWD peaks that was explained before. Accordingly, constraint (3a–d) were included so as to stipulate a maximum around x_1 and x_2 . Constraint (3e) and (f) were added in order to specify that the height of either of the

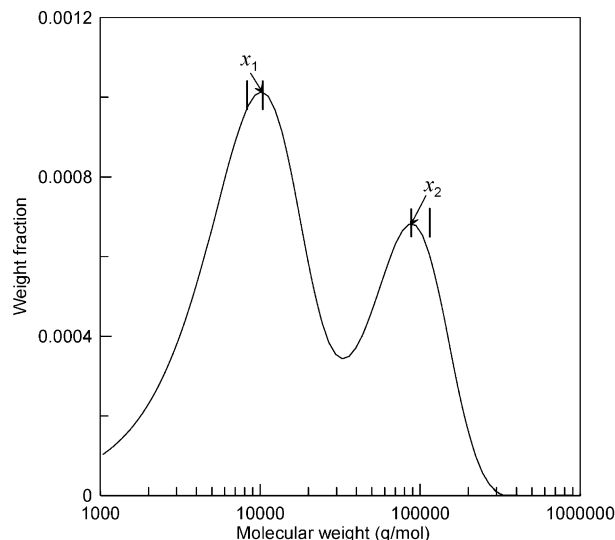


Figure 1. MWD at the reactor exit ($z = 63$ dm) corresponding to the optimal operating conditions of Optimization Problem 1. The vertical lines show the accepted intervals for the distribution peaks.

two peaks should be greater than a third of the other (representing a restriction on the relative mass fractions between the two peaks). Constraint (3g) and (h) are the permitted ranges for the positions of the MWD peaks. Constraint (3k-r) are the allowable bounds on process variables for the reactor set up considered here. Constraint (3j) specifies a minimum conversion at the reactor exit, in order to avoid optimization solutions that might yield unreasonably low conversions. Finally, constraint (3i) stipulates that the lateral feed position must be within the total reactor length (63 dm). It should be noted that only 6 points of the MWD, those corresponding to the chain lengths $x_1 - 5$, x_1 , $x_1 + 5$, $x_2 - 5$, x_2 , and $x_2 + 5$, needed to be included in the process model for solving the optimization problem. In this way, the size of the mathematical model could be kept fairly small.

As mentioned before, the optimization was carried out in gPROMS. Details about the optimization algorithm that was employed can be found elsewhere.^[19] The optimization process took 14 min using a PC with a Pentium IV processor and 1 Gb RAM, and the optimal point was:

$$z_{\text{lat}}^* = 41 \text{ dm}$$

$$x_1^* = 95, x_2^* = 850$$

$$f_{\text{St,main}}^* = 1.7 \frac{\text{g}}{\text{min}}, f_{\text{BPO,main}}^* = 0.0013 \frac{\text{g}}{\text{min}}, f_{\text{TEMPO,main}}^* = 0.00067 \frac{\text{g}}{\text{min}}$$

$$f_{\text{St,lat}}^* = 0.2 \frac{\text{g}}{\text{min}}, f_{\text{BPO,lat}}^* = 0.00197 \frac{\text{g}}{\text{min}}, f_{\text{TEMPO,lat}}^* = 0.0016 \frac{\text{g}}{\text{min}}$$

$$T^* = 135^\circ\text{C}, \text{ Total monomer flow rate} = 1.9 \frac{\text{g}}{\text{min}}$$

The bimodal MWD corresponding to the optimal point is shown in Figure 1. It can be seen that the target MWD is achieved, with peaks located as close to each other as the constraints for their positions allow it. Figure 2

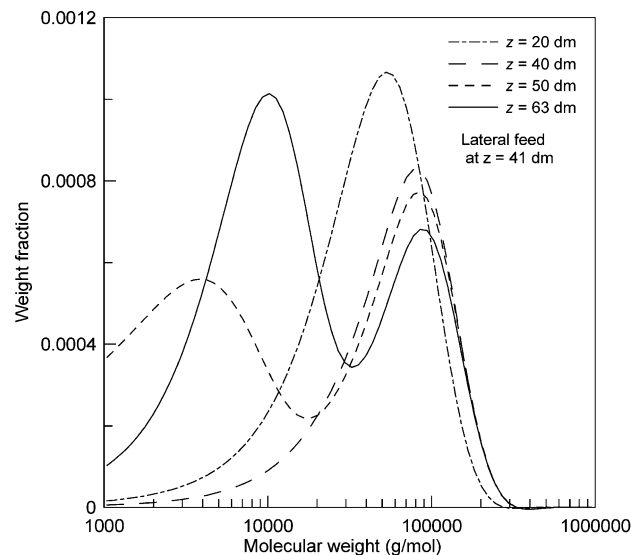


Figure 2. Evolution of the MWD along the tubular reactor axial distance for the optimal operating conditions of Optimization Problem 1.

shows the evolution of the MWD along the reactor axial distance. As expected, the reactants fed at the reactor inlet produce the high molecular weight peak of the distribution. This peak shifts towards higher molecular weights as the reaction mixture travels along the reactor, and the polymeric chains incorporate more monomer units. Notice that the MWD is unimodal before the lateral feed, and that at this point the distribution peak has almost reached the final position it will present at the reactor exit. The second lateral feed, located at $z = 41$ dm, leads to the low molecular weight peak. This peak also shifts to higher molecular weights as the polymeric chains grow in size along the reactor. It can be seen that the TEMPO flow rate in the lateral feed is much larger than that in the main feed. This aids in achieving the target low molecular weight, because a large number of new chains are introduced that compete for the available monomer.

The monomer conversion profile is shown in Figure 3, where it can be seen that the process requirement regarding this variable ($\text{conv} \geq 15\%$) is amply satisfied. The sudden drop in monomer conversion corresponds to the effect of the lateral feed. As the polymerization is performed in bulk, the monomer conversion of 30% would seem to be adequate for industrial conditions.

Optimization Problem 2

As a further test to the optimization approach for tailoring the MWD, the possibility of including a third peak to the bimodal distribution obtained in Optimization Problem 1 was analyzed, as proposed by Lenzi et al.^[5] This would be

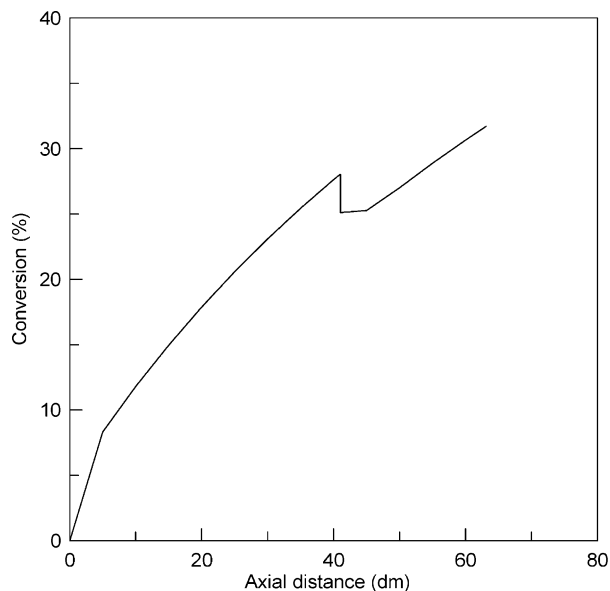


Figure 3. Conversion profile corresponding to the optimal operating conditions of Optimization Problem 1.

achieved by generating a third population of chains by means of an additional lateral feed. We established that the new peak should be placed between the chain lengths 350 and 550. It was intended to obtain a trimodal MWD with peak heights as similar as possible to each other. After trying different objective functions, it was finally decided to minimize the difference between the "deepness" of each peak relative to the nearest maximum [see the objective function in Equation (4)]. From a mathematical point of view, this optimization involved adding 7 new decision variables to the 10 of the previous optimization problem. The added decision variables were: location of the new lateral feed (z_{lat2}), flow rates of St, BPO and TEMPO for this feed ($f_{St,lat2}$, $f_{BPO,lat2}$, $f_{TEMPO,lat2}$), the chain length corresponding to the new peak (x_3), and the chain length corresponding to the local minimums (x_4 and x_5). The mathematical formulation of the optimization problem is presented in Equation (4). It is very similar to the one of the previous optimization problem [see Equation (3)]. Constraints were now included to specify maxima for x_1 [Equation (4a) and (b)], x_2 [Equation (4c) and (d)] and x_3 [Equation (4e) and (f)], and minima for x_4 [Equation (4g) and (h)] and x_5 [Equation (4i) and (j)]. Other constraints were incorporated so as to stipulate that the region of $x_4 \pm 5$ should be between the corresponding ones for x_1 and x_3 [(Equation (4k) and (l)), and equivalently for x_5 between x_3 and x_2 [Equation (4m) and (n)].

$$\begin{aligned}
 & \min_{z_{lat1}, z_{lat2}, x_1, x_2, x_3, x_4, x_5, f_{St,main}, f_{BPO,main}, f_{TEMPO,main}, f_{St,lat1}, f_{BPO,lat1}, f_{TEMPO,lat1}, f_{St,lat2}, f_{BPO,lat2}, f_{TEMPO,lat2}, T} \\
 & \text{s.t.} \\
 & \text{process model} \\
 & w(x_1 - 5) < w(x_1) \quad (a) \\
 & w(x_1 + 5) < w(x_1) \quad (b) \\
 & w(x_2 - 5) < w(x_2) \quad (c) \\
 & w(x_2 + 5) < w(x_2) \quad (d) \\
 & w(x_3 - 5) < w(x_3) \quad (e) \\
 & w(x_3 + 5) < w(x_3) \quad (f) \\
 & w(x_4) < w(x_4 - 5) \quad (g) \\
 & w(x_4) < w(x_4 + 5) \quad (h) \\
 & w(x_5) < w(x_5 - 5) \quad (i) \\
 & w(x_5) < w(x_5 + 5) \quad (j) \\
 & x_1 + 5 < x_4 - 5 \quad (k) \\
 & x_4 + 5 < x_3 - 5 \quad (l) \\
 & x_3 + 5 < x_5 - 5 \quad (m) \\
 & x_5 + 5 < x_2 - 5 \quad (n) \\
 & 85 \leq x_1 \leq 95 \quad (o) \\
 & 85 \leq x_4 \leq 550 \quad (p) \\
 & 350 \leq x_3 \leq 550 \quad (q) \\
 & 350 \leq x_5 \leq 1100 \quad (r) \\
 & 850 \leq x_2 \leq 1100 \quad (s) \\
 & 0 \leq z_{lat1} \leq 63 \text{ dm} \quad (t) \\
 & 0 \leq z_{lat2} \leq 63 \text{ dm} \quad (u)
 \end{aligned}$$

$$\text{FO} = \left(\begin{array}{l} \min((w(x_1) - w(x_4))^2, (w(x_3) - w(x_4))^2) \\ \min((w(x_3) - w(x_5))^2, (w(x_2) - w(x_5))^2) \end{array} \right)^2 \quad (4)$$

$$\begin{aligned}
 z_{\text{lat}2} - z_{\text{lat}1} &\geq 0 && \text{(v)} \\
 \text{conv} &\geq 15\% && \text{(w)} \\
 100^\circ\text{C} &\leq T \leq 135^\circ\text{C} && \text{(x)} \\
 0.5 \frac{\text{g}}{\text{min}} &\leq f_{\text{St},\text{main}} \leq 3.5 \frac{\text{g}}{\text{min}} && \text{(y)} \\
 0.0005 \frac{\text{g}}{\text{min}} &\leq f_{\text{BPO},\text{main}} \leq 0.006 \frac{\text{g}}{\text{min}} && \text{(z)} \\
 0.0001 \frac{\text{g}}{\text{min}} &\leq f_{\text{TEMPO},\text{main}} \leq 0.005 \frac{\text{g}}{\text{min}} && \text{(aa)} \\
 0.2 \frac{\text{g}}{\text{min}} &\leq f_{\text{St},\text{lat}1} \leq 3.5 \frac{\text{g}}{\text{min}} && \text{(ab)} \\
 0.0005 \frac{\text{g}}{\text{min}} &\leq f_{\text{BPO},\text{lat}1} \leq 0.01 \frac{\text{g}}{\text{min}} && \text{(ac)} \\
 0.0005 \frac{\text{g}}{\text{min}} &\leq f_{\text{TEMPO},\text{lat}1} \leq 0.01 \frac{\text{g}}{\text{min}} && \text{(ad)} \\
 0.2 \frac{\text{g}}{\text{min}} &\leq f_{\text{St},\text{lat}2} \leq 3.5 \frac{\text{g}}{\text{min}} && \text{(ae)} \\
 0.0005 \frac{\text{g}}{\text{min}} &\leq f_{\text{BPO},\text{lat}2} \leq 0.01 \frac{\text{g}}{\text{min}} && \text{(af)} \\
 0.0005 \frac{\text{g}}{\text{min}} &\leq f_{\text{TEMPO},\text{lat}2} \leq 0.01 \frac{\text{g}}{\text{min}} && \text{(ag)} \\
 1.9 \frac{\text{g}}{\text{min}} &\leq f_{\text{St},\text{main}} + f_{\text{St},\text{lat}1} + f_{\text{St},\text{lat}2} \leq 3.5 \frac{\text{g}}{\text{min}} && \text{(ah)}
 \end{aligned} \tag{4}$$

The mathematical model for the optimization included now 15 points of the MWD. The time required to solve the optimization was 17 min. The optimal point obtained was:

$$\begin{aligned}
 z_{\text{lat}1}^* &= 24.5 \text{ dm}, z_{\text{lat}2}^* = 46.5 \text{ dm} \\
 x_1^* &= 93, x_3^* = 408, x_2^* = 867 \\
 x_4^* &= 273, x_5^* = 611 \\
 f_{\text{St},\text{main}}^* &= 0.633 \frac{\text{g}}{\text{min}}, f_{\text{BPO},\text{main}}^* = 0.000527 \frac{\text{g}}{\text{min}}, f_{\text{TEMPO},\text{main}}^* = 0.000428 \frac{\text{g}}{\text{min}} \\
 f_{\text{St},\text{lat}1}^* &= 0.966 \frac{\text{g}}{\text{min}}, f_{\text{BPO},\text{lat}1}^* = 0.000654 \frac{\text{g}}{\text{min}}, f_{\text{TEMPO},\text{lat}1}^* = 0.0005 \frac{\text{g}}{\text{min}} \\
 f_{\text{St},\text{lat}2}^* &= 0.322 \frac{\text{g}}{\text{min}}, f_{\text{BPO},\text{lat}2}^* = 0.00179 \frac{\text{g}}{\text{min}}, f_{\text{TEMPO},\text{lat}2}^* = 0.00145 \frac{\text{g}}{\text{min}} \\
 T^* &= 134.7^\circ\text{C}, \text{Total monomer flow rate} = 1.921 \frac{\text{g}}{\text{min}}
 \end{aligned}$$

The resulting MWD is shown in Figure 4. It can be seen that the MWD is indeed trimodal, with the peaks located within the specified ranges. Parallelisms with respect to the previous process design can be observed. For instance, the reactor temperature and the total monomer flow rate are very similar. Also, the position and flow rates of the second lateral feed, responsible for the low molecular weight material, are alike. It can be noticed that, as in the previous case, the high molecular weight peak has almost reached its final position before the last lateral feed.

A difference that can be observed with respect to Optimization Problem 1 is that the monomer flow rate at the main feed, where the high molecular weight chains start growing, is smaller. This change can be explained by a long-enough residence time being needed before the 1st lateral feed, in order to allow a sufficient growth of the polymeric chains before the chains for the intermediate peak are added. Otherwise, these two chain populations would be too similar in size to yield two different peaks in the MWD. It can be seen in Figure 5 that monomer conversion is higher than 30% before the 1st lateral feed. Also notice from Figure 5 that the process constraint of a minimum conversion of 15% at the reactor exit is satisfied.

This analysis of the optimization solutions provides helpful guidelines on how to operate the controlled

polymerization in a tubular reactor in order to approach certain features of the MWD. However, the optimization methodology employed here is a very important tool because it provides the precise values of the different

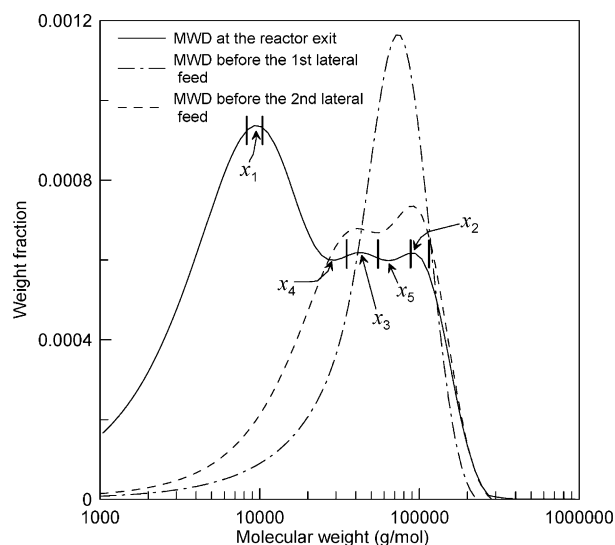


Figure 4. MWDs at the reactor exit ($z = 63$ dm), before the 2nd lateral feed ($z = 46.5$ dm) and before the 1st lateral feed ($z = 24.5$ dm) corresponding to the optimal operating conditions of Optimization Problem 2. The vertical lines show the accepted intervals for the distribution peaks.

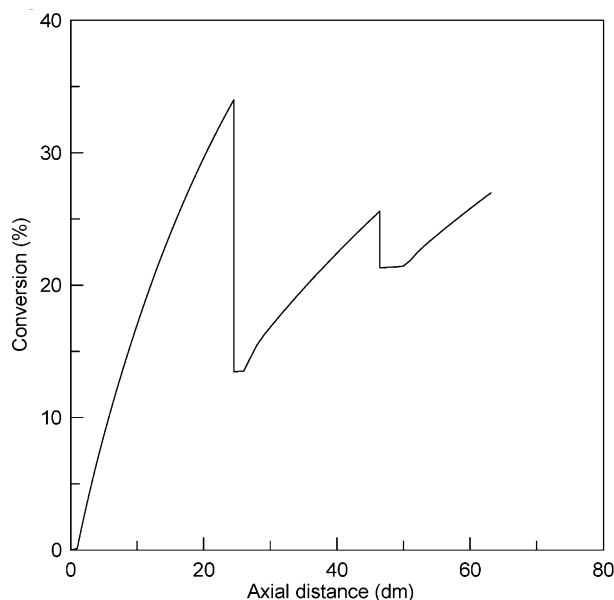


Figure 5. Conversion profile corresponding to the optimal operating conditions of Optimization Problem 2.

design and operating variables that would lead to the target MWDs.

Conclusion

A mathematical model of a nitroxide-mediated "living" radical polymerization in a tubular reactor, in which the complete molecular weight distribution is calculated using the probability generating function transformation, was used for the process optimization in order to obtain tailor-made MWDs. Multimodal distributions were obtained by generating populations of chains of different size by means of lateral feeds. Reactor temperature and the location of the feeds, as well as flow rates of styrene, initiator and nitroxide, were optimized in order to achieve tailor-made MWDs. In this way, it was shown that, by means of an efficient procedure, it was possible to find the precise set of operating conditions for producing polymers with complex MWD shapes, such as bimodal and trimodal distributions, with specific locations of the distribution peaks. As a consequence, it may be concluded that tubular reactors may be used successfully to perform controlled radical polymerizations and produce polymeric materials with unusual MWDs. The optimization approach presented in this work is applicable to other "living" radical systems, such as ATRP and RAFT, provided that a kinetic model is available. Although kinetic mechanisms for RAFT, ATRP and NMP involve different reactions, from the mathematical point of view, the mass balances of any of

them have the same structure. Therefore application of this technique to RAFT or ATRP systems is straightforward.

Acknowledgements: The authors wish to thank the *National Research Council of Argentina (CONICET)*, *Universidad Nacional del Sur, Bahía Blanca, Argentina (UNS)* and *Conselho Nacional de Desenvolvimento Científico e Tecnológico, Brazil (CNPq)* for financial support.

Received: February 22, 2008; Revised: April 12, 2008; Accepted: April 14, 2008; DOI: 10.1002/mren.200800015

Keywords: free radicals; living polymerization; modeling; molecular weight distribution; probability generating functions

- [1] K. Matyjaszewski, J. Spanswick, *Mater. Today* **2005**, *8*, 26.
- [2] K. Matyjaszewski, J. Xia, *Chem. Rev.* **2001**, *101*, 2921.
- [3] W. A. Braunecker, K. Matyjaszewski, *Prog. Polym. Sci.* **2007**, *32*, 93.
- [4] A. Goto, T. Fukuda, *Prog. Polym. Sci.* **2004**, *29*, 329.
- [5] M. K. Lenzi, M. F. Cunningham, E. L. Lima, J. C. Pinto, *Ind. Eng. Chem. Res.* **2005**, *44*, 2568.
- [6] A. A. M. Akerdi, A. Rabbani, S. Hakim, N. Fazeli, *Iran. Polym. J.* **2007**, *16*, 75.
- [7] US 6258504 B1, (2001), invs.: J. Bartus, R. Janules, J. Boswell, J. Clark.
- [8] N. Dan, M. Tirrell, *Macromolecules* **1993**, *26*, 6467.
- [9] M. Nele, A. Latado, J. C. Pinto, *Macromol. Mater. Eng.* **2006**, *291*, 272.
- [10] M. Nele, J. C. Pinto, *J. Appl. Polym. Sci.* **2000**, *77*, 437.
- [11] M. Nele, J. C. Pinto, *Macromol. Theory Simul.* **2002**, *11*, 293.
- [12] US 5548043 (1996), invs.: M. Saban, G. Liebermann, T. B. McAnaney.
- [13] M. Zhang, W. H. J. Ray, *J. Appl. Polym. Sci.* **2002**, *86*, 1047.
- [14] M. Zhang, W. H. J. Ray, *J. Appl. Polym. Sci.* **2002**, *86*, 1630.
- [15] A. Falijs, R. A. Yetter, C. A. Floudas, Y. Wei, H. Rabitz, *Polymer* **2001**, *42*, 2061.
- [16] T. E. Enright, M. F. Cunningham, B. Keoshkerian, *Macromol. Rapid Commun.* **2005**, *26*, 221.
- [17] J. P. Russum, PhD Thesis, Georgia Institute of Technology, USA 2005.
- [18] T. Noda, A. J. Grice, M. E. Levere, D. M. Haddleton, *Eur. Polym. J.* **2007**, *43*, 2321.
- [19] M. Asteasuain, M. Soares, M. K. Lenzi, M. Cunningham, C. Sarmoria, J. C. Pinto, A. Brandolin, *Macromol. React. Eng.* **2007**, *1*, 622.
- [20] P. A. Cabral, P. A. Melo, E. C. Biscaia, Jr, E. L. Lima, J. C. Pinto, *Polym. Eng. Sci.* **2003**, *43*, 1163.
- [21] M. P. Vega, E. L. Lima, J. C. Pinto, *Comput. Chem. Eng.* **1997**, *21*, S1049.
- [22] M. Asteasuain, A. Brandolin, C. Sarmoria, *Polymer* **2002**, *43*, 2529.
- [23] M. Asteasuain, C. Sarmoria, A. Brandolin, *Polymer* **2002**, *43*, 2513.
- [24] A. Brandolin, M. Asteasuain, C. Sarmoria, A. R. López, K. S. Whiteley, B. del Amo Fernández, *Polym. Eng. Sci.* **2001**, *41*, 1156.
- [25] M. Asteasuain, A. Brandolin, *Comput. Chem. Eng.* **2008**, *32*, 396.